Transp Porous Med (2010) 81:461–477
DOI 10.1007/s11242-009-9417-y

Convective Roll Instabilities of Vertical Throughflow with Viscous Dissipation in a Horizontal Porous Layer

Antonio Barletta · Eugenia Rossi di Schio · Leiv Storesletten

Received: 28 January 2009 / Accepted: 9 May 2009 / Published online: 13 June 2009

Abstract The vertical throughflow with viscous dissipation in a horizontal porous layer is studied. The horizontal plane boundaries are assumed to be isothermal with unequal temperatures and bottom heating. A basic stationary solution of the governing equations with a uniform vertical velocity field (throughflow) is determined. The temperature field in the basic solution depends only on the vertical coordinate. Departures from the linear heat conduction profile are displayed by the temperature distribution due to the forced convection effect and to the viscous dissipation effect. A linear stability analysis of the basic solution is carried out in order to determine the conditions for the onset of convective rolls. The critical values of the wave number and of the Darcy–Rayleigh number are determined numerically by the fourth-order Runge–Kutta method. It is shown that, although generally weak, the effect of viscous dissipation yields an increase of the critical value of the Darcy–Rayleigh number for downward throughflow and a decrease in the case of upward throughflow. Finally, the limiting case of a vanishing boundary temperature difference is discussed.

Keywords Porous medium · Darcy's law · Linear stability · Convective rolls · Throughflow

A. Barletta (✉) · E. Rossi di Schio
Dipartimento di Ingegneria Energetica, Nucleare e del Controllo Ambientale (DIENCA), Laboratorio di Montecuccolino, Alma Mater Studiorum Università di Bologna, via del Colli 16, 40136 Bologna, Italy
e-mail: antonio.barletta@unibo.it

E. Rossi di Schio
e-mail: eugenia.rossidischio@unibo.it

L. Storesletten
Department of Mathematics, University of Agder, Serviceboks 422, 4604 Kristiandsand, Norway
e-mail: leiv.storesletten@uia.no

1 Introduction

The viscous dissipation effect may be an important contribution in the energy balance of a fluid saturated porous medium (Nield 2007). This effect is specially significant when buoyant flow is coupled to a basic forced flow. Then, as pointed out in Chandrasekhar (1961), it is in forced or mixed convection processes that the heat generation due to viscous friction may be significant. On the other hand, in free convection, the viscous dissipation effect generally represents a higher order term within the framework of the Oberbeck–Boussinesq approximation. Chandrasekhar's reasoning refers to a clear fluid, but the same argument can be claimed, without substantial changes, also for fluid saturated porous media.

A few recent papers have investigated the effect of viscous dissipation with respect to the onset of convective instabilities either in clear fluids or in porous media (Mureithi and Mason 2002; Rees et al. 2005; Barletta et al. 2009). Mureithi and Mason (2002) study the convective linear instabilities induced by viscous dissipation for a boundary layer flow with an accelerating free-stream profile. Rees et al. (2005) carry out an analysis of the onset of transverse roll instabilities in a parallel external flow solution for the boundary layer around an inclined cold surface embedded in a porous medium. In a recent article by Barletta et al. (2009), the onset of convective instabilities in a horizontal porous layer with adiabatic bottom boundary and perfectly or imperfectly isothermal top boundary is investigated. In the basic solution considered by Barletta et al. (2009), the temperature gradient is built up solely as a consequence of the viscous dissipation in the porous medium. The study carried out by Barletta et al. (2009) has been extended by Storesletten and Barletta (2009) in order to describe the behaviour of cold water next to the maximum density temperature.

The analyses of the role of viscous dissipation in the onset of convective instabilities, carried out by Barletta et al. (2009) and Storesletten and Barletta (2009), deal with a horizontal basic flow through a porous layer. The objective of the present paper is to investigate the case of a basic vertical throughflow. Linear instabilities of a vertical throughflow in a horizontal porous layer have been investigated by several authors (Sutton 1970; Homsy and Sherwood 1976; Nield 1987; Khalili and Shivakumara 1998, 2003; Zhao et al. 1999). However, all these studies have been carried out without taking into account the effect of viscous dissipation. The interest for assessing the contribution of viscous dissipation in the study of throughflow in a horizontal porous layer and in the analysis of the onset of convective instabilities for this basic flow is the motivation of the present study. We mention that Sutton (1970) investigates the critical conditions for the onset of instabilities in a horizontal porous layer with lateral confinement by adiabatic boundaries. Homsy and Sherwood (1976) study the case of an infinitely wide plane horizontal channel bounded by isothermal horizontal boundaries. These authors carry out both a linear stability analysis and an energy stability analysis. Nield (1987) investigates other possible boundary conditions at the horizontal boundaries, thus extending the analysis of Homsy and Sherwood (1976). Khalili and Shivakumara (1998) further extend the analysis by including a uniform heat source within the porous layer. Zhao et al. (1999) consider a variant of the Homsy–Sherwood problem where the bottom boundary is subject to a uniform heat flux instead of a uniform temperature. Khalili and Shivakumara (2003) investigate non-Darcian effects in the analysis of the linear instabilities of vertical throughflow in a horizontal layer. They assume a general momentum balance where both the Brinkman term and the Forchheimer inertial term are included.

The aim of the present article is to revisit the Homsy–Sherwood problem (Homsy and Sherwood 1976) by taking into account the viscous dissipation term in the energy balance, in order to asses the effects of this contribution both in the basic throughflow solution and in the linear stability conditions for the onset of convective rolls.

Fig. 1 Porous layer

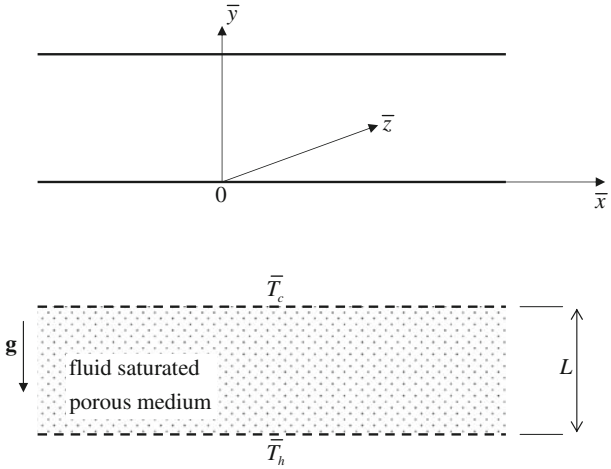

2 Mathematical Model

Let us consider a fluid saturated porous layer with thickness L. Let the vertical axis $\bar{y}$ be parallel to the gravitational acceleration $\mathbf{g}$, but with opposite direction (see Fig. 1). The boundary planes $\bar{y} = 0$ and $\bar{y} = L$ are kept isothermal at $\bar{T} = \bar{T}_h$ and $\bar{T} = \bar{T}_c$, respectively. Here $\bar{T}_h > \bar{T}_c$, and $\bar{T}$ denotes the temperature field. The velocity field $\bar{\mathbf{u}}$ has Cartesian components $(\bar{u}, \bar{v}, \bar{w})$.

2.1 Governing Equations

Let us assume the validity of Darcy's law, as well as of the Oberbeck–Boussinesq approximation. The effect of viscous dissipation is taken into account in the energy balance. We will adopt the c_v-formulation of the energy balance, also called internal-energy formulation, where c_v is the specific heat at constant volume. This formulation is suggested in Chandrasekhar (1961) as the most appropriate within the framework of the Oberbeck–Boussinesq approximation. A discussion of the internal-energy formulation and the enthalpy-formulation of the energy balance for buoyant flows is also carried out in Barletta (2008).

On account of the above assumptions, the local mass, momentum and energy balance yield the governing equations

$$\frac{\partial \bar{u}}{\partial \bar{x}} + \frac{\partial \bar{v}}{\partial \bar{y}} + \frac{\partial \bar{w}}{\partial \bar{z}} = 0, \tag{1}$$

$$\frac{\partial \bar{w}}{\partial \bar{y}} - \frac{\partial \bar{v}}{\partial \bar{z}} = -\frac{g\,\beta\,K}{\nu}\,\frac{\partial \bar{T}}{\partial \bar{z}}, \tag{2}$$

$$\frac{\partial \bar{u}}{\partial \bar{z}} - \frac{\partial \bar{w}}{\partial \bar{x}} = 0, \tag{3}$$

$$\frac{\partial \bar{v}}{\partial \bar{x}} - \frac{\partial \bar{u}}{\partial \bar{y}} = \frac{g\,\beta\,K}{\nu}\,\frac{\partial \bar{T}}{\partial \bar{x}}, \tag{4}$$

$$\sigma\,\frac{\partial \bar{T}}{\partial \bar{t}} + \bar{u}\,\frac{\partial \bar{T}}{\partial \bar{x}} + \bar{v}\,\frac{\partial \bar{T}}{\partial \bar{y}} + \bar{w}\,\frac{\partial \bar{T}}{\partial \bar{z}} = \alpha\left(\frac{\partial^2 \bar{T}}{\partial \bar{x}^2} + \frac{\partial^2 \bar{T}}{\partial \bar{y}^2} + \frac{\partial^2 \bar{T}}{\partial \bar{z}^2}\right) + \frac{\nu}{K\,c_v}\left(\bar{u}^2 + \bar{v}^2 + \bar{w}^2\right). \tag{5}$$

Equations 2–4 are the expressions of the three components of the vorticity evaluated starting from Darcy's law. In Eqs. 1–5, g is the modulus of $\mathbf{g}$, β is the coefficient of thermal expansion, K is the permeability, ν is the kinematic viscosity, $\bar{t}$ is time, σ is the ratio of the heat capacities of the fluid saturated porous medium and of the fluid and α is the effective thermal diffusivity of the fluid saturated porous medium.

A vertical throughflow is assumed, so that the boundary conditions are given by

$$\begin{aligned} \bar{y} = 0: \quad & \bar{v} = \bar{v}_0, \quad \bar{T} = \bar{T}_\mathrm{h}, \\ \bar{y} = L: \quad & \bar{v} = \bar{v}_0, \quad \bar{T} = \bar{T}_\mathrm{c}. \end{aligned} \tag{6}$$

2.2 Non-Dimensional Analysis

Let us introduce the following dimensionless quantities:

$$\begin{gathered} (x, y, z) = \frac{1}{L}\,(\bar{x}, \bar{y}, \bar{z})\,, \quad t = \frac{\alpha}{\sigma L^2}\,\bar{t}, \quad (u, v, w) = \frac{L}{\alpha}\,(\bar{u}, \bar{v}, \bar{w})\,, \\ T = \frac{\bar{T} - \bar{T}_\mathrm{c}}{\bar{T}_\mathrm{h} - \bar{T}_\mathrm{c}}, \quad \mathrm{Pe} = \frac{\bar{v}_0\, L}{\alpha}, \quad \mathrm{Ra} = \frac{g\,\beta\,L\,K(\bar{T}_\mathrm{h} - \bar{T}_\mathrm{c})}{\alpha\,\nu}, \\ \mathrm{Ge} = \frac{g\,\beta\,L}{c_\mathrm{v}}, \quad \mathrm{Ec} = \frac{\mathrm{Ge}}{\mathrm{Ra}} = \frac{\nu\,\alpha}{K\,c_\mathrm{v}\,(\bar{T}_\mathrm{h} - \bar{T}_\mathrm{c})}, \end{gathered} \tag{7}$$

where Ra and Ec are the Darcy–Rayleigh and the Darcy–Eckert numbers, Pe is the Péclet number and Ge is the Gebhart (or dissipation) number. We note that, while Ra, Ec and Ge can only be positive, the Péclet number can be either positive (*upward throughflow*) or negative (*downward throughflow*).

By employing the dimensionless quantities, Eqs. 1–6 can be rewritten as follows:

$$\frac{\partial u}{\partial x} + \frac{\partial v}{\partial y} + \frac{\partial w}{\partial z} = 0, \tag{8}$$

$$\frac{\partial w}{\partial y} - \frac{\partial v}{\partial z} = -\,\mathrm{Ra}\,\frac{\partial T}{\partial z}, \tag{9}$$

$$\frac{\partial u}{\partial z} - \frac{\partial w}{\partial x} = 0, \tag{10}$$

$$\frac{\partial v}{\partial x} - \frac{\partial u}{\partial y} = \mathrm{Ra}\,\frac{\partial T}{\partial x}, \tag{11}$$

$$\frac{\partial T}{\partial t} + u\,\frac{\partial T}{\partial x} + v\,\frac{\partial T}{\partial y} + w\,\frac{\partial T}{\partial z} = \frac{\partial^2 T}{\partial x^2} + \frac{\partial^2 T}{\partial y^2} + \frac{\partial^2 T}{\partial z^2} + \mathrm{Ec}\left(u^2 + v^2 + w^2\right), \tag{12}$$

$$\begin{aligned} y = 0: \quad & v = \mathrm{Pe}, \quad T = 1, \\ y = 1: \quad & v = \mathrm{Pe}, \quad T = 0. \end{aligned} \tag{13}$$

2.3 Basic Solution

A basic stationary solution of Eqs. 8–13 is given by a uniform throughflow,

$$u_B = 0, \quad v_B = \mathrm{Pe}, \quad w_B = 0, \tag{14}$$

with a purely vertical temperature gradient $\mathrm{d}T_B(y)/\mathrm{d}y$. Here, the subscript B stands for "basic". On account of Eqs. 12–14, the basic temperature distribution $T_B(y)$ must satisfy the differential equation

$$\frac{\mathrm{d}^2 T_B}{\mathrm{d}y^2} - \mathrm{Pe}\,\frac{\mathrm{d}T_B}{\mathrm{d}y} + \mathrm{Ec}\,\mathrm{Pe}^2 = 0, \tag{15}$$

together with the boundary conditions

$$T_B(0) = 1, \quad T_B(1) = 0. \tag{16}$$

The solution is given by

$$T_B(y) = \frac{\mathrm{e}^{\mathrm{Pe}} - \mathrm{e}^{\mathrm{Pe}\,y}}{\mathrm{e}^{\mathrm{Pe}} - 1} + \mathrm{Ec}\,\mathrm{Pe}\left(y - \frac{\mathrm{e}^{\mathrm{Pe}\,y} - 1}{\mathrm{e}^{\mathrm{Pe}} - 1}\right). \tag{17}$$

2.4 Linear Disturbances

Let us assume the following perturbation of the basic solution:

$$u = u_B + \varepsilon\, U, \quad v = v_B + \varepsilon\, V, \quad w = w_B + \varepsilon\, W, \quad T = T_B + \varepsilon\, \theta, \tag{18}$$

where $\varepsilon \ll 1$ is a small parameter. We substitute Eq. 18 into Eqs. 8–13 and neglect the terms proportional to ε^2. Then, we obtain

$$\frac{\partial U}{\partial x} + \frac{\partial V}{\partial y} + \frac{\partial W}{\partial z} = 0, \tag{19}$$

$$\frac{\partial W}{\partial y} - \frac{\partial V}{\partial z} = -\,\mathrm{Ra}\,\frac{\partial \theta}{\partial z}, \tag{20}$$

$$\frac{\partial U}{\partial z} - \frac{\partial W}{\partial x} = 0, \tag{21}$$

$$\frac{\partial V}{\partial x} - \frac{\partial U}{\partial y} = \mathrm{Ra}\,\frac{\partial \theta}{\partial x}, \tag{22}$$

$$\frac{\partial \theta}{\partial t} + V\,\frac{\mathrm{d}T_B}{\mathrm{d}y} + \mathrm{Pe}\,\frac{\partial \theta}{\partial y} = \frac{\partial^2 \theta}{\partial x^2} + \frac{\partial^2 \theta}{\partial y^2} + \frac{\partial^2 \theta}{\partial z^2} + 2\,\mathrm{Ec}\,\mathrm{Pe}\,V, \tag{23}$$

$$\begin{aligned} y = 0: &\quad V = 0, \quad \theta = 0, \\ y = 1: &\quad V = 0, \quad \theta = 0. \end{aligned} \tag{24}$$

3 Stability Analysis

We now consider disturbances in the form of plane waves. Due to the linearity of our analysis, an arbitrary disturbance can be properly constructed by a superposition of these plane waves.

3.1 Disturbance Equations

The geometry, the boundary conditions and the basic solution of the governing equations are invariant under rotations around any axis parallel to the y-direction. Due to this symmetry, the propagation direction of the plane wave disturbance can be any horizontal direction. It is not restrictive to assume this direction as that of the x-axis. Then, the analysis of the linear disturbances becomes two-dimensional with

$$U = U(x, y, t), \quad V = V(x, y, t), \quad W = 0, \quad \theta = \theta(x, y, t). \tag{25}$$

On account of Eq. 25, we infer that Eqs. 20 and 21 are identically satisfied, Eq. 19 is fulfilled provided that we express U and V by means of a streamfunction ψ, namely,

$$U = \frac{\partial \psi}{\partial y}, \quad V = -\frac{\partial \psi}{\partial x}. \tag{26}$$

Now, Eqs. 22–24 can be rewritten as

$$\frac{\partial^2 \psi}{\partial x^2} + \frac{\partial^2 \psi}{\partial y^2} = -\mathrm{Ra}\, \frac{\partial \theta}{\partial x}, \tag{27}$$

$$\frac{\partial \theta}{\partial t} + \mathrm{Pe}\, \frac{\partial \theta}{\partial y} = \frac{\partial^2 \theta}{\partial x^2} + \frac{\partial^2 \theta}{\partial y^2} - \mathrm{Pe}\, F(y)\, \frac{\partial \psi}{\partial x}, \tag{28}$$

$$y = 0, 1: \quad \psi = 0, \quad \theta = 0, \tag{29}$$

where $F(y)$ is defined as

$$F(y) = -\frac{1}{\mathrm{Pe}}\, \frac{\mathrm{d}T_B}{\mathrm{d}y} + 2\,\mathrm{Ec} = \frac{\mathrm{e}^{\mathrm{Pe}\, y}}{\mathrm{e}^{\mathrm{Pe}} - 1} + \mathrm{Ec} \left(1 + \mathrm{Pe}\, \frac{\mathrm{e}^{\mathrm{Pe}\, y}}{\mathrm{e}^{\mathrm{Pe}} - 1} \right) \tag{30}$$

We are seeking solutions of Eqs. 27–30 in the form of plane waves,

$$\psi(x,\ y,\ t) = \Psi(y)\, \mathrm{e}^{\lambda t}\, \cos(a\, x), \quad \theta(x,\ y,\ t) = \Theta(y)\, \mathrm{e}^{\lambda t}\, \sin(a\, x), \tag{31}$$

where a is the wave number and λ is the coefficient of exponential time growth. In order to investigate the condition of marginal stability, we will fix $\lambda = 0$. Then, by substituting Eq. 31 into Eqs. 27–29 one obtains

$$\Psi'' - a^2\, \Psi + a\, \mathrm{Ra}\, \Theta = 0, \tag{32}$$

$$\Theta'' - \mathrm{Pe}\, \Theta' - a^2 \Theta + a\, \mathrm{Pe}\, F(y)\, \Psi = 0, \tag{33}$$

$$y = 0, 1: \quad \Psi = 0, \quad \Theta = 0, \tag{34}$$

where the primes denote differentiation with respect to y.

It is easily proved from Eq. 30 that, in the absence of viscous dissipation, i.e. for $\mathrm{Ec} = 0$ or $\mathrm{Ge} = 0$, the transformation $\{y \to 1 - y, \mathrm{Pe} \to -\mathrm{Pe}\}$ implies $F \to -F$. Then, for $\mathrm{Ec} = 0$ or $\mathrm{Ge} = 0$, Eqs. 32–34 are left invariant by the transformation $\{y \to 1 - y, \mathrm{Pe} \to -\mathrm{Pe}\}$ provided that both a and Ra are left unchanged. A special consequence of this invariance is that the critical values of a and Ra do not depend on the sign of Pe, i.e. on the direction of the throughflow, when viscous dissipation is negligible, $\mathrm{Ec} = 0$ or $\mathrm{Ge} = 0$. On the other hand, this symmetry is broken if viscous dissipation is taken into account ($\mathrm{Ec} \neq 0$ and $\mathrm{Ge} \neq 0$).

3.2 Numerical Solution

We seek a numerical solution of Eqs. 32–34 by considering this differential problem as an eigenvalue problem. More precisely, we assume Pe and Ge to be prescribed and then, we determine the eigenvalue Ra corresponding to each a such that a non-trivial solution of Eqs. 32–34 exists. This procedure yields a function $\mathrm{Ra}(a)$ describing the marginal stability curve in the parametric plane (a, Ra). As is well-known, the critical values a_{cr} and $\mathrm{Ra}_{\mathrm{cr}}$ are determined by seeking the minimum of the function $\mathrm{Ra}(a)$.

A proper numerical procedure is based on the fourth-order Runge–Kutta method. In order to use this method, we need to formulate the differential problem as an initial-value problem. In fact, we can replace Eq. 34 with

Table 1 Comparison between the Runge–Kutta method with fixed step size h and the Runge-Kutta method with variable step size determined through an adaptive algorithm. Critical values of Ra (in roman) and a (in *italic*) for Ge = 1 and different Pe

Pe	$h = 10^{-1}$	$h = 10^{-2}$	$h = 10^{-4}$	$h = 10^{-5}$	Adaptive
5	62.148074	62.148058	62.148051	62.148054	62.148055
	4.0591247	*4.0591262*	*4.0591266*	*4.0591265*	*4.0591265*
6	73.237111	73.237035	73.237024	73.237028	73.237028
	4.4954728	*4.4954807*	*4.4954814*	*4.4954813*	*4.4954813*
7	85.505253	85.504950	85.504930	85.504937	85.504937
	5.0336308	*5.0336659*	*5.0336675*	*5.0336672*	*5.0336672*
8	98.442492	98.441414	98.441380	98.441390	98.441391
	5.6649106	*5.6650480*	*5.6650512*	*5.6650507*	*5.6650507*
9	111.68907	111.68565	111.68560	111.68561	111.68561
	6.3637437	*6.3642115*	*6.3642174*	*6.3642167*	*6.3642167*
10	125.05336	125.04360	125.04351	125.04353	125.04353
	7.1000405	*7.1014355*	*7.1014455*	*7.1014445*	*7.1014445*

$$\Psi(0) = 0, \quad \Psi'(0) = 1, \quad \Theta(0) = 0, \quad \Theta'(0) = \xi. \tag{35}$$

The condition on $\Psi'(0)$ is due to the following reason. Since the differential problem Eqs. 32–34 is homogeneous, then any non-trivial solution can be arbitrarily rescaled yielding another solution. Thus, we can encompass this scaling freedom by the constraint $\Psi'(0) = 1$. In Eq. 35, ξ is a yet unknown constant. For any given a, Pe and Ge, the value of ξ together with the eigenvalue Ra is determined by prescribing the boundary conditions at $y = 1$, namely,

$$\Psi(1) = 0, \quad \Theta(1) = 0. \tag{36}$$

We point out that the choice to fix Ge instead of fixing directly the value of Ec is due to the dependence of Ec on the boundary temperature difference, i.e. $\bar{T}_h - \bar{T}_c$. Indeed, when searching the eigenvalues Ra, we aim to determine the marginal stability values of the temperature difference between the boundary planes. Thus, in this procedure, it appears as incoherent to assume as prescribed the value of a parameter, Ec, which depends on the marginal stability values of $\bar{T}_\mathrm{h} - \bar{T}_\mathrm{c}$.

The fourth-order explicit Runge–Kutta method is easily implemented by means of the function `NDSolve` available within the software environment *Mathematica 7.0* (©Wolfram Research). The numerical values obtained through this procedure can be validated by determining the effect on the results of the chosen step-size h employed in the computation. This analysis is reported in Table 1, where the critical values a_cr and Ra_cr corresponding to Ge = 1 and $5 \leq \mathrm{Pe} \leq 10$, respectively, are given for different decreasing step-sizes h. The last column reported in Table 1 yields the values of a_cr and Ra_cr obtained by the explicit Runge–Kutta method with adaptive step-size control. The default settings of function `NDSolve` imply an adaptive step-size control by the embedded pairs algorithm, which produces at each step a changing h. The comparison between the results obtained with the lowest step-size $h = 10^{-5}$ and those determined with the adaptive step-size control reveals an excellent agreement. This test justifies the choice of the adaptive step-size control for the explicit Runge–Kutta method in all subsequent computations.

4 Discussion of the Results

4.1 Forced Convection Throughflow and Viscous Dissipation

As is well-known, if the velocity of the vertical throughflow was zero in the basic state, then the basic temperature profile would be the conduction profile $T_B(y) = 1 - y$. This elementary result can be formally inferred from Eq. 17 by evaluating the limit $\mathrm{Pe} \to 0$. A peculiar consequence of the upward throughflow ($\mathrm{Pe} > 0$) is that the forced convection heat transfer produces a global temperature increase with respect to the conduction profile. The reverse occurs in the case of downward throughflow ($\mathrm{Pe} < 0$). The physical reason of this behaviour is simple: the porous layer experiences a hot fluid input when $\mathrm{Pe} > 0$, while cold fluid seeps through the layer when $\mathrm{Pe} < 0$. This straightforward effect is made more complicated by viscous dissipation. In fact, viscous dissipation produces an additional heating within the layer independently of the throughflow direction, i.e., whatever is the sign of Pe. In the case of upward throughflow ($\mathrm{Pe} > 0$), both viscous dissipation and forced convection contribute to the system heating. In the case of downward throughflow ($\mathrm{Pe} < 0$), viscous dissipation and forced convection are competing effects: viscous dissipation can prevail over the cooling action of forced convection only if it is sufficiently intense, namely, if Ec is sufficiently large. There is a condition such that the competing actions of viscous dissipation and forced convection are perfectly balanced. This condition is $\mathrm{Ec}\,\mathrm{Pe} = -1$. In fact, one may easily verify from Eq. 17 that, whatever are the values of Ec and Pe such that $\mathrm{Ec}\,\mathrm{Pe} = -1$, the basic temperature profile becomes the conduction profile, $T_B(y) = 1 - y$.

The above described behaviour of the temperature distribution in the basic flow is illustrated in Fig. 2. This figure shows clearly that an increasing value of Ec yields a global increase in the temperature at every position y, both for $\mathrm{Pe} = -15$ and for $\mathrm{Pe} = 15$. The linear conduction profile is clearly displayed in the upper frame, in the case $\mathrm{Ec} = 1/15$. The upper frame shows also that temperatures higher than the bottom boundary temperature may exist for a sufficiently high Ec: this behaviour is evident for $\mathrm{Ec} = 0.08, 0.1$. The threshold value of Ec for this effect to occur is easily determined by means of Eq. 17 by prescribing that the derivative $\mathrm{d}T_B/\mathrm{d}y$ vanishes at $y = 0$. In this way, one concludes that the porous layer may display temperatures higher than the bottom boundary temperature if

$$\mathrm{Ec} > \frac{1}{\mathrm{e}^{\mathrm{Pe}} - \mathrm{Pe} - 1}. \tag{37}$$

For $\mathrm{Pe} = -15$, this means $\mathrm{Ec} > 0.0714286$. For $\mathrm{Pe} = 15$, Eq. 37 yields $\mathrm{Ec} > 3.05904 \times 10^{-7}$. The latter result justifies the behaviour displayed by the plots with $\mathrm{Ec} = 0.08, 0.1$ in the upper frame of Fig. 2, and by all the plots in the lower frame of Fig. 2, which correspond to $\mathrm{Ec} \geq 0.03$.

4.2 Onset of Convective Rolls

In Tables 2 and 3, the critical values of a and Ra for the onset of convective rolls are reported for different Péclet and Gebhart numbers. Table 2 refers to downward throughflow ($\mathrm{Pe} < 0$), while Table 3 refers to upward throughflow ($\mathrm{Pe} > 0$). These tables reveal that, while a_{cr} and $\mathrm{Ra}_{\mathrm{cr}}$ depend significantly on Pe, they depend weakly on Ge. The effect of Ge depends on the direction of throughflow. If $\mathrm{Pe} < 0$ (Table 2), one may note that the values of a_{cr} and $\mathrm{Ra}_{\mathrm{cr}}$ increase with Ge. If $\mathrm{Pe} > 0$ (Table 3), the values of a_{cr} and $\mathrm{Ra}_{\mathrm{cr}}$ decrease with Ge. In other words, viscous dissipation has a weak stabilizing effect for downward throughflow and

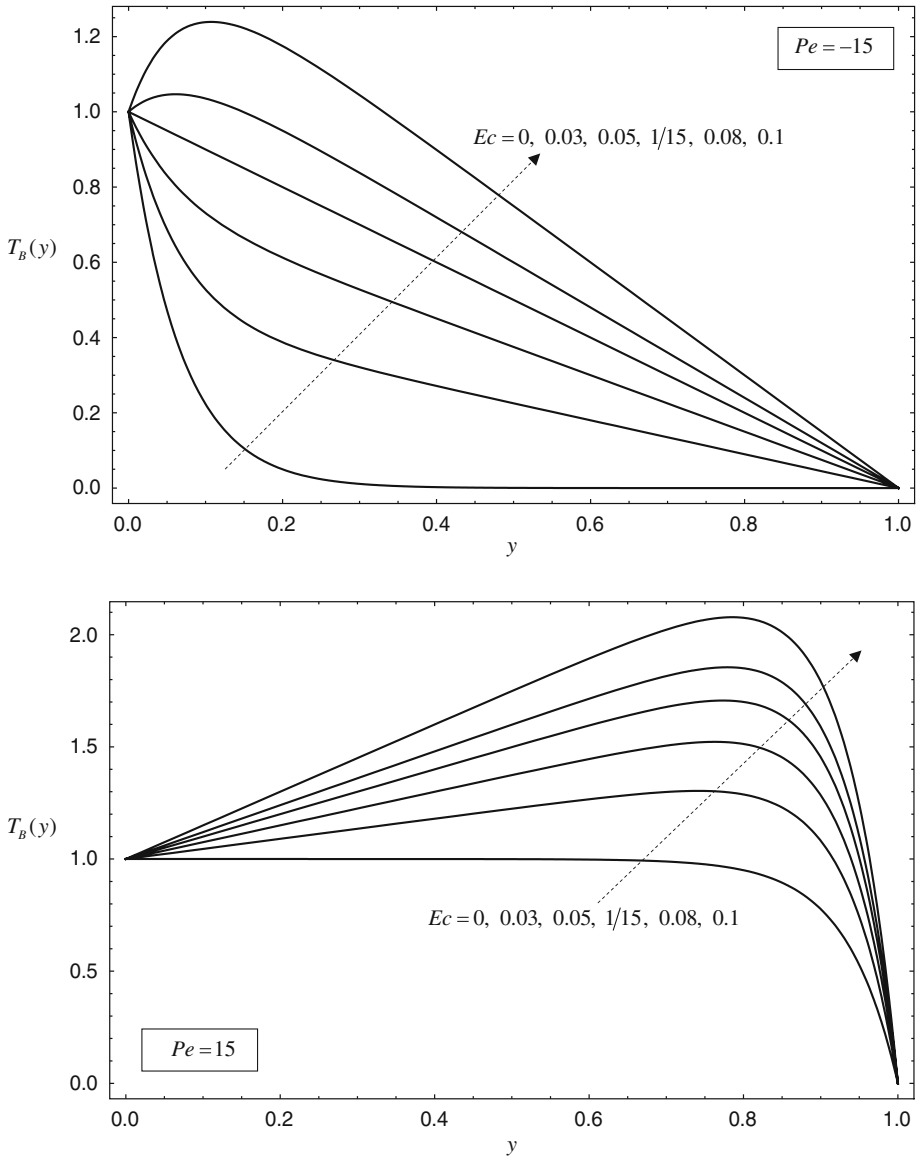

Fig. 2 Plots of $T_B(y)$ for different values of Ec; the upper frame refers to Pe $= -15$ and the lower frame to Pe $= 15$

a weak destabilizing effect for upward throughflow. This conclusion implies the breaking of the symmetry between downward and upward throughflow described in Sect. 3.1.

In general, a more intense throughflow (a higher |Pe|) implies increasing values of a_{cr} and $\mathrm{Ra}_{\mathrm{cr}}$. A weak violation of this rule is observed in Table 3 for high values of Ge and very small values of Pe. In this range, we observe that $\mathrm{Ra}_{\mathrm{cr}}$ initially decreases with Pe, reaches a minimum and then starts increasing. It must be pointed out that this effect is definitely a minor one. A visual representation of the data reported in Tables 2 and 3 is given in

Table 2 Downward throughflow (Pe < 0). Critical values of Ra (in roman) and a (in *italic*)

Pe	Ge $= 0$	Ge $= 10^{-5}$	Ge $= 10^{-2}$	Ge $= 10^{-1}$	Ge $= 1/2$	Ge $= 1$
-10^{-3}	39.4784	39.4784	39.4784	39.4786	39.4794	39.4804
	3.14159	*3.14159*	*3.14159*	*3.14159*	*3.14159*	*3.14159*
-10^{-2}	39.4786	39.4786	39.4788	39.4806	39.4886	39.4986
	3.14160	*3.14160*	*3.14160*	*3.14160*	*3.14160*	*3.14160*
-10^{-1}	39.4924	39.4924	39.4944	39.5124	39.5924	39.6924
	3.14196	*3.14196*	*3.14196*	*3.14196*	*3.14196*	*3.14196*
-1	40.8751	40.8751	40.8953	41.0770	41.8848	42.8945
	3.17868	*3.17868*	*3.17868*	*3.17876*	*3.17912*	*3.17956*
-2	45.0776	45.0777	45.1191	45.4922	47.1499	49.2208
	3.29218	*3.29218*	*3.29225*	*3.29292*	*3.29591*	*3.29973*
-3	52.0684	52.0685	52.1327	52.7114	55.2797	58.4824
	3.48965	*3.48965*	*3.48992*	*3.49235*	*3.50333*	*3.51747*
-4	61.6664	61.6665	61.7546	62.5472	66.0580	70.4183
	3.78501	*3.78501*	*3.78571*	*3.79197*	*3.82042*	*3.85729*
-5	73.4146	73.4147	73.5256	74.5231	78.9249	84.3558
	4.19616	*4.19616*	*4.19759*	*4.21053*	*4.26904*	*4.34423*
-6	86.6192	86.6193	86.7497	87.9218	93.0718	99.3812
	4.73292	*4.73293*	*4.73534*	*4.75709*	*4.85385*	*4.97402*
-7	100.581	100.581	100.727	102.036	107.773	114.775
	5.37860	*5.37861*	*5.38193*	*5.41179*	*5.54128*	*5.69529*
-8	114.833	114.833	114.991	116.410	122.628	130.220
	6.09212	*6.09213*	*6.09604*	*6.13095*	*6.27960*	*6.45151*
-9	129.167	129.167	129.336	130.853	137.506	145.645
	6.83594	*6.83594*	*6.84013*	*6.87743*	*7.03495*	*7.21531*
-10	143.518	143.519	143.698	145.307	152.377	161.048
	7.59035	*7.59036*	*7.59465*	*7.63292*	*7.79436*	*7.97919*
-15	215.283	215.283	215.512	217.574	226.680	237.942
	11.3830	*11.3830*	*11.3874*	*11.4263*	*11.5928*	*11.7877*

Figs. 3 and 4. These figures display a comparison between the values of $a_{\rm cr}$ and $\mathrm{Ra}_{\rm cr}$ for the case Ge $= 0$ and those for the case Ge $= 1$. In Figs. 3 and 4, the data for Ge $= 0$ are also compared with the correlations obtained by Homsy and Sherwood (1976) for $|\mathrm{Pe}| \gg 1$,

$$a_{\rm cr} \cong 0.759\,|\mathrm{Pe}|, \quad \mathrm{Ra}_{\rm cr} \cong 14.3\,|\mathrm{Pe}|, \tag{38}$$

in the absence of viscous dissipation. From Figs. 3 and 4, one may see that these correlations are in very good agreement with the evaluated data for Ge $= 0$, provided that $|\mathrm{Pe}| \gtrsim 7$. These figures reveal also the above described breaking of the symmetry Pe $\to -$Pe in the case Ge $= 1$. As expected, the curves of $a_{\rm cr}$ and $\mathrm{Ra}_{\rm cr}$ for either Ge $= 0$ or Ge $= 1$ tend to

$$a_{\rm cr} = \pi, \quad \mathrm{Ra}_{\rm cr} = 4\,\pi^2, \tag{39}$$

when $|\mathrm{Pe}| \to 0$, i.e. in the absence of throughflow. As is well-known, the critical values reported in Eq. 39 are those of the Darcy–Bénard problem (Nield and Bejan 2006; Rees

Table 3 Upward throughflow (Pe > 0). Critical values of Ra (in roman) and a (in *italic*)

Pe	Ge = 0	Ge = 10^{-5}	Ge = 10^{-2}	Ge = 10^{-1}	Ge = 1/2	Ge = 1
10^{-3}	39.4784	39.4784	39.4784	39.4782	39.4774	39.4764
	3.14159	*3.14159*	*3.14159*	*3.14159*	*3.14159*	*3.14159*
10^{-2}	39.4786	39.4786	39.4784	39.4766	39.4686	39.4586
	3.14160	*3.14160*	*3.14160*	*3.14160*	*3.14160*	*3.14160*
10^{-1}	39.4924	39.4924	39.4904	39.4724	39.3924	39.2923
	3.14196	*3.14196*	*3.14196*	*3.14196*	*3.14196*	*3.14196*
1	40.8751	40.8751	40.8549	40.6731	39.8652	38.8553
	3.17868	*3.17868*	*3.17867*	*3.17859*	*3.17824*	*3.17781*
2	45.0776	45.0776	45.0361	44.6630	43.0038	40.9286
	3.29218	*3.29218*	*3.29211*	*3.29144*	*3.28853*	*3.28496*
3	52.0684	52.0684	52.0041	51.4251	48.8485	45.6201
	3.48965	*3.48965*	*3.48938*	*3.48697*	*3.47643*	*3.46366*
4	61.6664	61.6663	61.5783	60.7844	57.2436	52.7896
	3.78501	*3.78501*	*3.78432*	*3.77811*	*3.75112*	*3.71875*
5	73.4146	73.4144	73.3035	72.3028	67.8228	62.1480
	4.19616	*4.19616*	*4.19473*	*4.18191*	*4.12606*	*4.05913*
6	86.6192	86.6191	86.4886	85.3104	80.0113	73.2370
	4.73292	*4.73292*	*4.73051*	*4.70879*	*4.61287*	*4.49548*
7	100.581	100.581	100.435	99.1172	93.1696	85.5049
	5.37860	*5.37860*	*5.37527*	*5.34512*	*5.20854*	*5.03367*
8	114.833	114.832	114.674	113.245	106.789	98.4414
	6.09212	*6.09212*	*6.08820*	*6.05260*	*5.88744*	*5.66505*
9	129.167	129.167	128.998	127.471	120.582	111.686
	6.83594	*6.83593*	*6.83174*	*6.79354*	*6.61402*	*6.36422*
10	143.518	143.518	143.339	141.721	134.428	125.044
	7.59035	*7.59035*	*7.58604*	*7.54682*	*7.36187*	*7.10144*
15	215.283	215.283	215.053	212.985	203.727	191.985
	11.3830	*11.3830*	*11.3786*	*11.3390*	*11.1549*	*10.9036*

2000; Tyvand 2002). The latter is the special case of the present problem for a vanishing throughflow velocity (Pe = 0). When Pe = 0, the viscous dissipation has no influence on the linear stability analysis as it would manifest itself in an intrinsically nonlinear term, quadratic in the disturbance velocity components. One may easily check this reasoning by evaluating the limit Pe → 0 in Eq. 23 and noticing that the resulting equation is independent of Ec.

4.3 Vanishing Difference Between the Boundary Temperatures

As it has been pointed out in the preceding sections, the convective instabilities within the porous layer are, in general, a result of two causes. The first cause is the positive temperature difference $\bar{T}_h - \bar{T}_c$ between the bottom and the top boundary planes. The second cause is the heat generation within the layer due to the viscous dissipation effect. We know from the Homsy and Sherwood analysis (Homsy and Sherwood 1976), as well as from our results

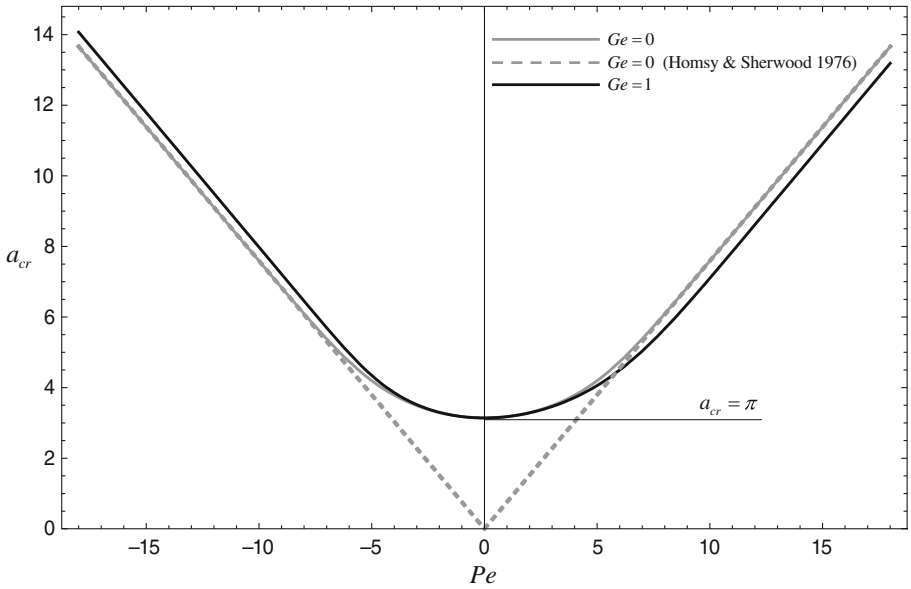

Fig. 3 Plots of $a_{\rm cr}$ versus Pe

obtained for Ge $\to$ 0, that the first cause alone is capable of generating convective instabilities. This happens when the second cause, i.e. viscous dissipation, is negligible. We now pose a different question. If the first cause becomes negligible, i.e. if $\bar{T}_{\rm h} - \bar{T}_{\rm c} \to 0$, is viscous dissipation alone capable of generating convective instabilities in the porous layer?

The answer to this question requires that we reconsider the eigenvalue problem Eqs. 32–34 in the limit Ec $\to \infty$ (or Ra $\to$ 0). In this limit, we want the following quantities to remain finite:

$$\tilde{\Theta} = {\rm Ec}^{-1}\,\Theta, \quad \tilde{\Psi} = {\rm Pe}\,\Psi, \quad \tilde{F}(y) = {\rm Ec}^{-1}\,F(y), \quad \Lambda = {\rm Ge}\,{\rm Pe}. \tag{40}$$

From Eqs. 7, 18 and 40, we note that Λ and all tilded quantities are independent of $\bar{T}_{\rm h} - \bar{T}_{\rm c}$. Let us now take the limit Ec $\to \infty$. Equation 30 yields

$$\tilde{F}(y) = 1 + {\rm Pe}\,\frac{{\rm e}^{{\rm Pe}\,y}}{{\rm e}^{\rm Pe} - 1}, \tag{41}$$

while Eqs. 32–34 can be rewritten as

$$\tilde{\Psi}'' - a^2\,\tilde{\Psi} + a\,\Lambda\,\tilde{\Theta} = 0, \tag{42}$$

$$\tilde{\Theta}'' - {\rm Pe}\,\tilde{\Theta}' - a^2\tilde{\Theta} + a\,\tilde{F}(y)\,\tilde{\Psi} = 0, \tag{43}$$

$$y = 0, 1: \quad \tilde{\Psi} = 0, \quad \tilde{\Theta} = 0. \tag{44}$$

Equations 42 and 44 can be solved by fixing $(a, {\rm Pe})$ and determining Λ as an eigenvalue. The numerical procedure followed to solve the eigenvalue problem is that described in Sect. 3.2. After defining the function $\Lambda(a)$, one can determine the critical values $(a_{\rm cr}, \Lambda_{\rm cr})$, for each fixed Pe, by seeking the minimum of $\Lambda(a)$. From Eq. 41, one may easily verify that Eqs. 42–44 are left invariant by the transformation

$$y \to 1 - y, \quad {\rm Pe} \to -{\rm Pe}. \tag{45}$$

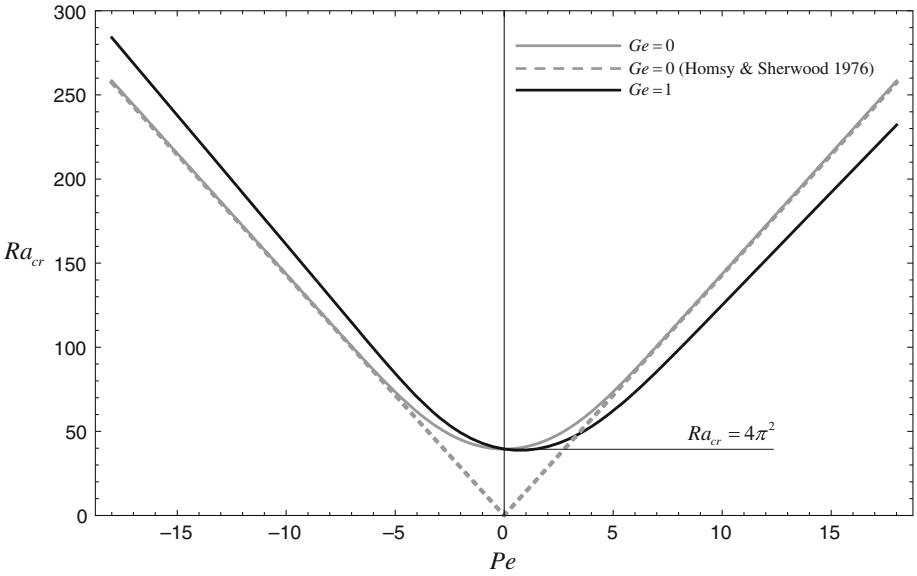

Fig. 4 Plots of $\mathrm{Ra_{cr}}$ versus Pe

This means that the pair $(a_{\mathrm{cr}}, \Lambda_{\mathrm{cr}})$ is independent of the sign of Pe. However, the data reported in Table 4 reveal that, for every prescribed Pe, the values of Λ_{cr} are always positive. This implies that convective instabilities can occur only in the case of upward throughflow (Pe $>$ 0). In fact, if Pe $<$ 0, Eq. 40 implies that a positive Λ_{cr} means a negative Ge, i.e. an impossible condition. Hence, in the limit Ec $\to \infty$, downward throughflow is linearly stable for every Pe. On the other hand, viscous dissipation alone may generate convective instabilities in the case of upward throughflow.

Table 4 shows that both a_{cr} and Λ_{cr} are increasing functions of Pe. This table suggests that, for Pe $\to$ 0, both a_{cr} and Λ_{cr} attain a finite limit. In the Appendix, it is shown that for Pe $\to$ 0 one has

$$a_{\mathrm{cr}} = \pi \cong 3.14159, \quad \Lambda_{\mathrm{cr}} = 2\pi^2 \cong 19.7392. \tag{46}$$

These values are consistent with the data for small Pe reported in Table 4. We note that the value $\Lambda_{\mathrm{cr}} \cong 19.7392$ attained for values of Pe smaller than 10^{-2} corresponds in fact to huge values of the Gebhart number, $\mathrm{Ge} = \Lambda/\mathrm{Pe}$. As a consequence, its interest is purely theoretical. In the large-Pe regime, the asymptotic procedure described in the Appendix shows that, in the limit Pe $\to \infty$, one has the critical values

$$a_{\mathrm{cr}} = 6.06793, \quad \mathrm{Ge_{cr}} = 4.67910. \tag{47}$$

This means that, in the large-Pe regime, Λ_{cr} becomes a linear function of Pe. One may easily check that a fairly linear behaviour of Λ_{cr} versus Pe is displayed by the values reported in Table 4 for Pe $\geq$ 20. Equation 47 has an important meaning. The upward throughflow may develop convective instabilities inasmuch as Ge $>$ 4.67910. No instabilities can occur for smaller values of Ge, no matter how large is Pe. The threshold value Ge $=$ 4.67910 is extremely large. We mention that Turcotte et al. (1974) develop an analysis for very large values of the Gebhart number, called by these authors dissipation number. However, they do

Table 4 Upward throughflow (Pe > 0) with Ec $\to \infty$. Critical values of a and Λ

Pe	a_{cr}	Λ_{cr}	Pe	a_{cr}	Λ_{cr}
10^{-5}	3.14159	19.7392	10	4.17840	52.8218
10^{-4}	3.14159	19.7392	11	4.26194	57.7604
10^{-3}	3.14159	19.7392	12	4.33599	62.7284
10^{-2}	3.14159	19.7393	13	4.40228	67.7025
10^{-1}	3.14183	19.7439	14	4.46232	72.6674
1	3.16469	20.2065	15	4.51733	77.6139
3/2	3.19281	20.7845	16	4.56825	82.5375
2	3.23086	21.5824	17	4.61578	87.4362
5/2	3.27762	22.5895	18	4.66040	92.3104
3	3.33169	23.7927	19	4.70249	97.1611
4	3.45567	26.7265	20	4.74233	101.990
5	3.59092	30.2544	21	4.78012	106.800
6	3.72723	34.2473	22	4.81603	111.592
7	3.85728	38.5891	23	4.85021	116.368
8	3.97670	43.1819	24	4.88276	121.131
9	4.08372	47.9467	25	4.91380	125.882

not consider values above Ge $= 3$. Thus, we can conclude that convective instabilities of upward throughflow purely driven by viscous dissipation do not occur in practical cases.

5 Conclusions

The effect of viscous dissipation has been taken into account in the analysis of vertical throughflow in a horizontal porous layer saturated by a fluid. The plane boundaries of the layer are kept isothermal with unequal temperatures and bottom heating. The basic solution of the problem is a vertical uniform throughflow directed either upward or downward. The temperature in the basic state depends only on the vertical coordinate. The temperature distribution differs, in general, from the linear heat conduction profile due to the forced convection induced by the throughflow and to the viscous dissipation effect. The governing parameters of the basic solution are the Péclet number Pe associated to the throughflow and the ratio between the Gebhart number Ge and the Darcy-Rayleigh number Ra, i.e. the Darcy–Eckert number Ec. The main features of the basic solution have been studied. Moreover, a linear stability analysis of the basic solution has been carried out for the onset of convective rolls. The critical values of the wave number and of the Darcy–Rayleigh number have been obtained by a numerical procedure based on the fourth-order Runge–Kutta method with an adaptive step-size control by the embedded pairs algorithm. The main inferences drawn from the present investigation are resumed as follows.

- In the basic solution with downward throughflow, the forced convection due to the throughflow and viscous dissipation are competing effects. The former yields a cooling effect in the system, while the latter yields an internal heating of the layer. The competition may result in a perfect balance between these effects when Ec Pe $= -1$. In this case, the basic temperature profile is the linear heat conduction profile.

- The effect of viscous dissipation breaks the symmetry between downward and upward throughflow with respect to the critical conditions for the onset of convective instabilities.
- Although generally weak, the effect of viscous dissipation is stabilizing in the case of downward throughflow and destabilizing in the case of upward throughflow.
- While the critical values $\mathrm{Ra}_{\mathrm{cr}}$ and a_{cr} at onset of convection depend significantly on Pe, they depend weakly on Ge.
- In general, a more intense throughflow (a higher |Pe|) implies increasing values of $\mathrm{Ra}_{\mathrm{cr}}$ and a_{cr}.
- Convective instabilities of upward throughflow are theoretically predicted also in the special case $\bar{T}_{\mathrm{h}} - \bar{T}_{\mathrm{c}} = 0$. These instabilities are caused solely by the effect of viscous dissipation. It has been shown that they exist only if $\mathrm{Ge} > 4.67910$. Since the threshold value of Ge is very high and the value of Ge is very low in practical problems, this kind of instabilities has a purely mathematical interest. In the case of downward throughflow, instabilities caused solely by the effect of viscous dissipation do not exist.

Appendix

Vanishing Difference Between the Boundary Temperatures: Limit $\mathrm{Pe} \to 0$

The conditions $\mathrm{Ec} \to \infty$ and $\mathrm{Pe} \to 0$ are assumed. When $\mathrm{Pe} \to 0$, Eq. 41 yields $\tilde{F}(y) = 2$. Then, in this limit, Eqs. 42–44 can be simplified to

$$\tilde{\Psi}'' - a^2\,\tilde{\Psi} + a\,\Lambda\,\tilde{\Theta} = 0, \tag{48}$$

$$\tilde{\Theta}'' - a^2\tilde{\Theta} + 2\,a\,\tilde{\Psi} = 0, \tag{49}$$

$$y = 0, 1: \quad \tilde{\Psi} = 0, \quad \tilde{\Theta} = 0. \tag{50}$$

A solution of Eqs. 48–50 can be sought in the form

$$\tilde{\Psi}(y) = A\,\sin(n\,\pi\,y), \quad \tilde{\Theta}(y) = B\,\sin(n\,\pi\,y). \tag{51}$$

Equation 51 identically satisfies Eq. 50 for every positive integer n. By substituting Eq. 51 in Eqs. 48 and 49, one obtains

$$[(n\,\pi)^2 + a^2]\,A - a\,\Lambda\,B = 0, \tag{52}$$

$$[(n\,\pi)^2 + a^2]\,B - 2\,a\,A = 0. \tag{53}$$

One may easily show that Eqs. 52 and 53 are fulfilled for arbitrary values of A and B provided that

$$\Lambda = \frac{[(n\,\pi)^2 + a^2]^2}{2\,a^2}. \tag{54}$$

Among the marginal stability curves $\Lambda(a)$ defined by Eq. 54, the lowest one is that for $n = 1$. This curve admits a minimum for $a = \pi$, corresponding to $\Lambda = 2\,\pi^2$.

Vanishing Difference Between the Boundary Temperatures: Limit $\mathrm{Pe} \to \infty$

The conditions $\mathrm{Ec} \to \infty$ and $\mathrm{Pe} \to \infty$ are assumed. Let us reconsider Eqs. 42–44 by adopting $\Psi = \tilde{\Psi}/\mathrm{Pe}$ instead of $\tilde{\Psi}$. For every y such that $0 \le y < 1$, one may easily evaluate the limit $\tilde{F}(y)$ for $\mathrm{Pe} \to +\infty$.

$$\lim_{\mathrm{Pe}\to+\infty}\tilde{F}(y)=\lim_{\mathrm{Pe}\to+\infty}\left(1+\mathrm{Pe}\,\frac{\mathrm{e}^{\mathrm{Pe}\,y}}{\mathrm{e}^{\mathrm{Pe}}-1}\right)=1+\lim_{\mathrm{Pe}\to+\infty}\left[\mathrm{Pe}\,\frac{\mathrm{e}^{-\mathrm{Pe}\,(1-y)}}{1-\mathrm{e}^{-\mathrm{Pe}}}\right]=1. \tag{55}$$

As a consequence, Eq. 43 yields

$$\tilde{\Theta}''-\mathrm{Pe}\,\tilde{\Theta}'-a^2\tilde{\Theta}+a\,\mathrm{Pe}\,\Psi=0, \tag{56}$$

and, in the limit $\mathrm{Pe}\to+\infty$, it can be approximated by the lower order equation

$$\tilde{\Theta}'-a\,\Psi=0. \tag{57}$$

Obviously, the reduction in the order of Eq. 56 implies that one of the two boundary conditions on Θ, expressed by Eq. 44, cannot be fulfilled. Since the limit of $\tilde{F}(y)$, evaluated in Eq. 55, is finite only for $y\neq 1$, then the boundary condition $\tilde{\Theta}(1)=0$ becomes incompatible with Eq. 57. Equations 42–44 now read

$$\Psi''-a^2\,\Psi+a\,\mathrm{Ge}\,\tilde{\Theta}=0, \tag{58}$$

$$\tilde{\Theta}'-a\,\Psi=0, \tag{59}$$

$$\Psi(0)=0,\quad \tilde{\Theta}(0)=0,\quad \Psi(1)=0, \tag{60}$$

where use has been made of the definition $\Lambda=\mathrm{Ge}\,\mathrm{Pe}$. Equations 58 and 60 imply the additional boundary condition $\Psi''(0)=0$. Therefore, by differentiating Eq. 58 with respect to y and by using Eq. 59, one obtains

$$\Psi'''-a^2\,\Psi'+a^2\,\mathrm{Ge}\,\Psi=0, \tag{61}$$

$$\Psi(0)=0,\quad \Psi''(0)=0,\quad \Psi(1)=0. \tag{62}$$

Adapting the numerical procedure described in Sect. 3.2, one may determine the eigenvalue $\mathrm{Ge}(a)$ corresponding to any prescribed wave number a. Finally, by seeking the minimum of function $\mathrm{Ge}(a)$, one obtains the critical values

$$a_{\mathrm{cr}}\cong 6.06793,\quad \mathrm{Ge}_{\mathrm{cr}}\cong 4.67910. \tag{63}$$

References

Barletta, A.: Comments on a paradox of viscous dissipation and its relation to the Oberbeck–Boussinesq approach. Int. J. Heat Mass Transf. **51**, 6312–6316 (2008)

Barletta, A., Celli, M., Rees, D.A.S.: The onset of convection in a porous layer induced by viscous dissipation: a linear stability analysis. Int. J. Heat Mass Transf. **52**, 337–344 (2009)

Chandrasekhar, S.: Hydrodynamic and Hydromagnetic Stability. Oxford University Press, Oxford (1961)

Homsy, G.M., Sherwood, A.E.: Convective instabilities in porous media with through flow. AIChE J. **22**, 168–174 (1976)

Khalili, A., Shivakumara, I.S.: Onset of convection in a porous layer with net through-flow and internal heat generation. Phys. Fluids **10**, 315–317 (1998)

Khalili, A., Shivakumara, I.S.: Non-Darcian effects on the onset of convection in a porous layer with throughflow. Transp. Porous Media **53**, 245–263 (2003)

Mureithi, E.W., Mason, D.P.: On the stability of a forced-free boundary layer flow with viscous heating. Fluid Dyn. Res. **31**, 65–78 (2002)

Nield, D.A.: Convective instabilities in porous media with throughflow. AIChE J. **33**, 1222–1224 (1987)

Nield, D.A.: The modeling of viscous dissipation in a saturated porous medium. ASME J. Heat Transf. **129**, 1459–1463 (2007)

Nield, D.A., Bejan, A.: Convection in Porous Media, 3rd edn. Springer, Berlin (2006)

Rees, D.A.S.: The Stability of Darcy–Bénard convection. In: Vafai, K. (ed.) Handbook of Porous Media, pp. 521–558. Marcel Dekker, New York (2000)
Rees, D.A.S., Magyari, E., Keller, B.: Vortex instability of the asymptotic dissipation profile in a porous medium. Transp. Porous Media **61**, 1–14 (2005)
Storesletten, L., Barletta, A.: Linear instability of mixed convection of cold water in a porous layer induced by viscous dissipation. Int. J. Thermal Sci. **48**, 655–664 (2009)
Sutton, F.M.: Onset of convection in a porous channel with net through flow. Phys. Fluids **13**, 1931–1934 (1970)
Turcotte, D.L., Hsui, A.T., Torrance, K.E., Schubert, G.: Influence of viscous dissipation on Bénard convection. J. Fluid Mech. **64**, 369–374 (1974)
Tyvand, P.A.: Onset of Rayleigh–Bénard convection in porous bodies. In: Ingham, D.B., Pop, I. (eds.) Transport Phenomena in Porous Media II, pp. 82–112. Elsevier, Pergamon, Oxford (2002)
Zhao, C., Hobbs, B.E., Mühlhaus, H.B.: Theoretical and numerical analyses of convective instability in porous media with upward throughflow. Int. J. Numer. Anal. Meth. Geomech. **23**, 629–646 (1999)